Observations and Modeling of the Relation Between Effective Reservoir Stress and Hydraulic Fracture Propagation Pressure

de Pater, Hans; Prabhakaran, Rahul; Shaoul, Josef

DOI
10.2118/184831-MS

Publication date
2017

Document Version
Final published version

Published in
Proceedings of the SPE Hydraulic Fracturing Technology Conference and Exhibition

SPE-184831-MS

Observations and Modeling of the Relation Between Effective Reservoir Stress and Hydraulic Fracture Propagation Pressure

C. J. de Pater, Fenix Consulting Delft; R. Prabhakaran, TU Delft; J. R. Shaoul, Fenix Consulting Delft

This paper was prepared for presentation at the SPE Hydraulic Fracturing Technology Conference and Exhibition held in The Woodlands, Texas, USA, 24-26 January 2017.

Abstract

Accurate prediction of net hydraulic fracture propagation pressure is often impossible. Under some conditions the pressure drop along the fracture dominates while in other cases the pressure at the tip determines the net pressure. Properly scaled lab tests and modeling indicate that effective stress determines the tip propagation pressure, but this is hard to confirm with field data in specific cases.

We therefore gathered a large data base of fracture treatments from many areas to investigate the correlation between net pressure and effective stress. In order to avoid any spurious effect from fluid friction, tortuosity and height containment we limited the data to relatively small injections with water or linear gel in vertical wells. All treatments were in conventional clastic reservoirs, but over a large range of permeability, rock stiffness and geological age.

The data show a remarkably good correlation between net pressure and effective reservoir stress, with a slope of 0.46. Lower net pressure of 200-300 psi was found in over pressured reservoirs and higher net pressure of about 1500 psi was seen in depleted reservoirs. We checked that this is not due to another underlying parameter, such as modulus or depth, which could explain the correlation. It is concluded that the correlation is due to a true relation between net pressure (controlled by fracture propagation) and effective stress. Simulation of representative treatments with a new model that includes a cohesive zone at the fracture tip shows excellent agreement with the observed correlation, supporting a physical relation.

The relation between net pressure and effective stress in the reservoir can contribute to improved treatment design in green fields and also will aid in understanding fracture height growth, since effective stress will differ between formation layers. Calibrated models will still be important in view of lack of detailed formation knowledge, but a correct description of the physics of fracture propagation, based on effective stress at the tip, will facilitate more accurate model predictions.

Introduction

Net fracture propagation pressure (net pressure) is fundamental to understanding fracture geometry, in particular height growth. However, it is often impossible to accurately predict net pressure a priori from formation and pumping parameters. In conventional fracture modeling, as embedded in industry software, the minimum stress is the reference level for fracture pressure, but pore pressure is absent in the description, except in the fluid leak-off model.

The formation elasticity, fluid viscosity and injection rate, together with the dimensions of the fracture determine net pressure. The propagation condition is assumed to derive from linear elastic fracture mechanics which compares the tensile opening force (given by fracture pressure minus minimum stress) with a critical toughness which is a rock parameter. It has been proposed that toughness depends on effective stress, which would introduce pore pressure in an indirect way. But toughness values measured in the laboratory are still much too small to explain high net pressures.

A more fundamental way to look at propagation is based on the characteristics of rock failure, which does not yield a sharp fracture tip, but a cohesive zone with failure of intact rock ahead of the cohesive zone given by effective tensile stress exceeding the strength. Such a mechanism has been confirmed in lab tests where it was essential for a correct description of the fluid lag at the fracture tip (van Dam et al, 2001, 2002). For practical purposes the most important consequence of this mechanism is that in deep formations, strength (fracture toughness) becomes insignificant compared with the difference between stress and pore pressure. Conversely, the effective strength of rock would be quite low in over pressured reservoirs where the difference between stress and pore pressure can be quite low. Also, in water flooding, a relatively low net pressure is expected since pore pressure is enhanced around the fracture, while the enhanced stress does not fully compensate the increased pore pressure.

Therefore a crucial test on the proposed propagation mechanism is the observed relation between pore pressure and net fracture propagation pressure: pore pressure should have a large effect. Discerning the effect in actual field data is however complicated by other effects of pore pressure that are well known. Reservoir depletion can yield a stress contrast that contains fractures which will increase net pressure. Depletion will also enhance fluid leak-off, giving small fractures that have relatively high net pressure due to low compliance. Even indirect effects can play a role, since high reservoir pressure (and minimum stress) will result in high injection pressure, which can lead to opening up out-of-plane fractures and the resulting fracture complexity can also increase net pressure.

Methodology

Fracture Treatment Analysis

To investigate the pore pressure effect, treatments were selected that would show minimal effects from factors such as tortuosity, fluid friction changes by proppant and fracture height containment. It is well known that apparent net pressure can be influenced by other factors than the true fracture propagation pressure. In order to discern any effect of pore pressure, the influence of other factors should be minimized. Only those wells that have an inclination of 10 degrees or below are chosen for the analysis. This is to eliminate the effect of fracture complexity and near-wellbore tortuosity that can occur when fractures initiates from wellbore perforation orientation and then re-align to the preferred fracture plane orientation. The basis for this threshold is experimental studies on differences between perforation orientation and minimum stress direction (Behrmann et al, 1992; Abass et al, 1994; Weijers, 1995). In order to eliminate the effects of fluid friction owing to fluid viscosity, proppant transport and tip screen-out, only breakdown and minifrac injection Instantaneous Shut-in Pressures (ISIP's) were initially considered for the analysis.

A total of 421 datafrac treatments spanning 13 fields were analyzed to investigate the pore pressure effect, see Table 1. The treatments include a wide range of reservoir depths, reservoir pressures, geological settings and geological age. All the fields however were clastics from different depositional environments. Since most of the cases involved two datafrac injections (breakdown and minifrac) followed by the main propped fracture treatment, the main treatment pressure data (additional 215 jobs) was also collected for comparison with the level of net pressure from the datafracs. Using the Instantaneous Shut-in Pressure (ISIP) from the measured pressure data and the closure stress obtained using the graphical method from G-Function plots

(Nolte, 1979), the net pressure ISIP was obtained for each treatment. Using this value and the reservoir pressure data, the Terzaghi minimum principal effective stress was also calculated.

Table 1—Fracture jobs classified by field, depositional environment, geological age and type of treatment

Field	Depositional Environment	Geological Age	Break Down	Mini Frac	Main Frac	Total
A	Fluvial - Shallow Marine	Cambro-Ordovician	14	14	14	42
B	Turbidite	Lower Miocene	6	5	5	16
C	Turbidite	Oligocene	0	1	1	2
D	Fluvial-Lacustrine-Shallow Marine	Triassic	18	18	18	54
E	Fluvial-Lacustrine-Shallow Marine	Triassic	13	17	15	45
F	Fluvial	Triassic	3	3	3	9
G	Paralic / Marine	Devonian	2	2	2	6
H	Open Marine, Deep Shelf/ Deltaic - Shallow Marine	Early Miocene / Middle Oligocene	8	9	7	24
I	Fluvial Plain – Deltaic / Aeolian	Carboniferous / Permian	3	3	3	9
J	Fluvial - Shallow Marine	Ordovician	4	5	3	12
K	Fluvial - Aeolian Dune - Inter Dune/ Lacustrine-Sabkha	Permian	2	2	2	6
L	Deep Marine	Cretaceous	72	60	69	201
M	Fluvial–Marginal Marine	Cambrian-Ordovician	74	61	73	208
			219	200	215	634

Plotting closure stress gradient against pore pressure gradient as in Figure 1, it can be observed that the selection covers a wide range of reservoir pressure scenarios. It is evident that the high pressured reservoirs also have a high stress gradient. All the treatments were performed in the past 20 years. Some of the fields were extremely faulted & compartmentalized and hence had considerable pore pressure variation over relatively small areas. Some data points correspond to fields under secondary recovery and in which injection wells were fracture stimulated.

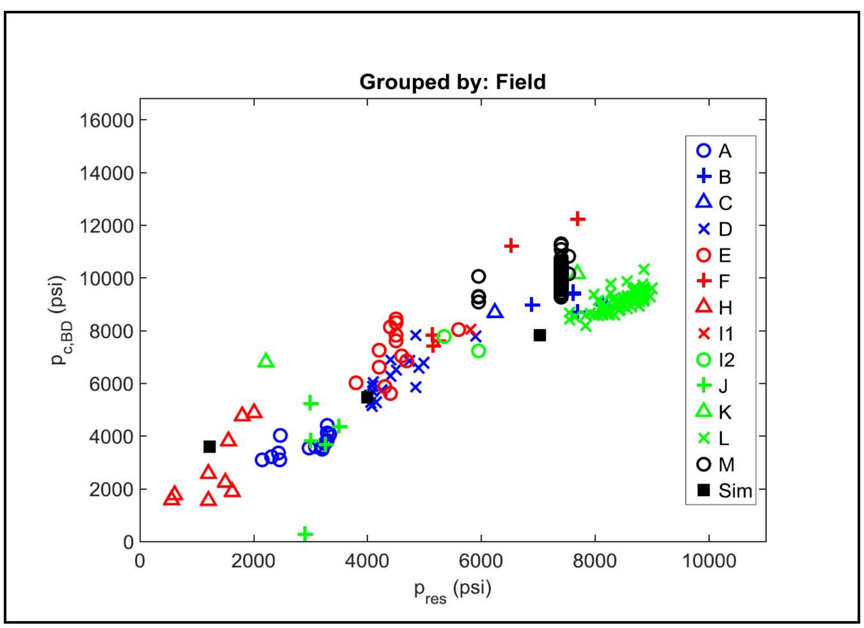

Figure 1—Closure pressure from decline after breakdown injections vs. reservoir pressure.

The minimum principal stress variation with depth is depicted in Figure 2, together with a typical minimum stress gradient of 0.7 psi/ft for a normally pressured reservoir without tectonic effects. In the case of Fields B, F and L, the minimum principal stress is much higher.

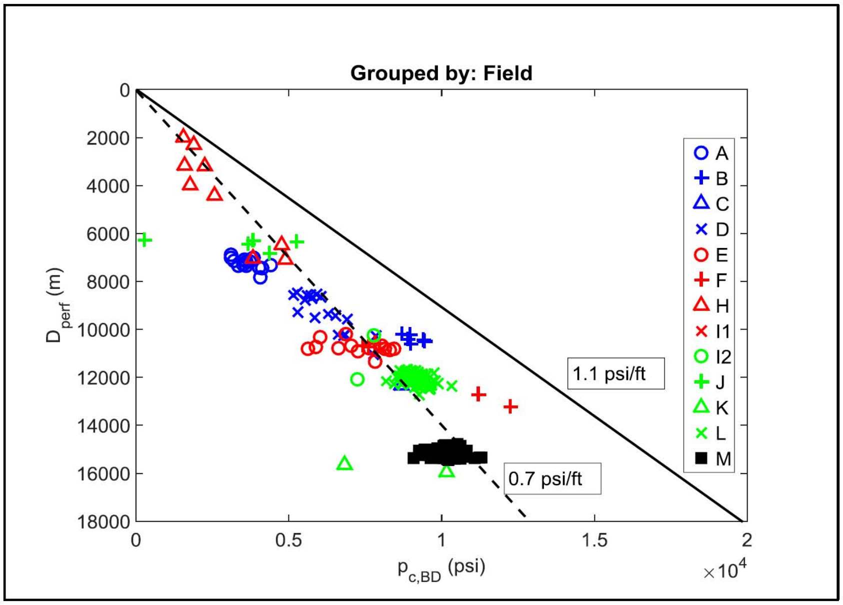

Figure 2—Closure pressure with depth for all treatments grouped by Field.

Reservoir pressure with depth is shown in Figure 3. Fields A, E and H are sub-hydrostatic. Fields B and L are over pressured. Figure 4 shows effective minimum stress with depth. A relatively large difference is observed in the case of Field E, F and H. Deep reservoirs will generally also have high effective stress that is expected to show up in high net pressure. Figure 5 shows that minimum stress gradient in the pay correlates with reservoir pressure gradient. In this plot two effects appear: higher stress in over pressured reservoirs and stress variation in a reservoir caused by depletion.

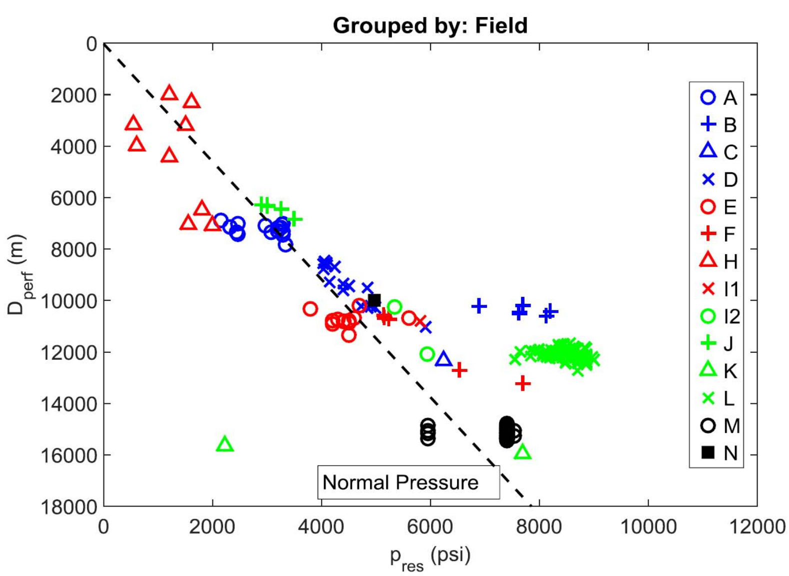

Figure 3—Reservoir pressure with depth for all treatments grouped by Field.

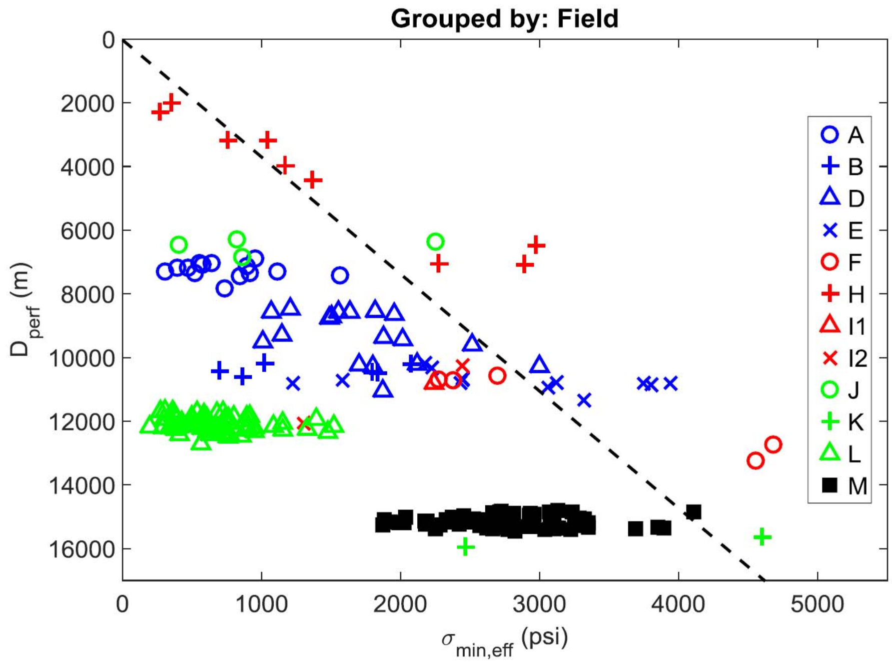

Figure 4—Effective minimum stress with depth for all treatments grouped by Field. The dashed line indicates normally pressured fields with stress gradient of 0.7 psi/ft.

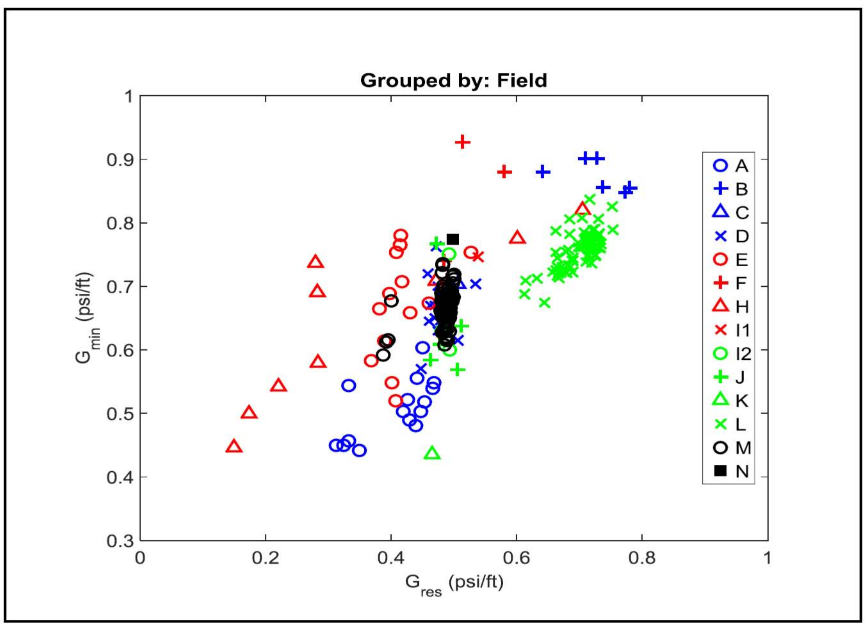

Figure 5—Minimum stress Gradient in the Pay vs. Reservoir Pressure Gradient for all treatments grouped by Field. The dashed line indicates expected stress variation of reservoirs with stress gradient of 0.7 psi/ft and stress path coefficient of 0.5.

As can be seen in Figure 4, the minimum effective principal stress varies within the treatments from the same field. Therefore, the collection of treatments should provide independent data on the effect of depth and the effect of reservoir pressure on the value of net pressure.

Synthetic Test Cases

Using the range of parameters from the treatment analysis, four synthetic reservoir test cases were formulated. The reservoir is approximated as a three layer system with a pay zone bounded by overlying and underlying shales. The first three synthetic cases represent under pressured, hydrostatic and over pressured reservoirs. The fourth synthetic case represents a high effective stress reservoir in which there is a large difference between the pore pressure and closure stress. The first three synthetic cases utilize a common reservoir geometry and geomechanical property description. This was obtained using the statistical mean from the reservoir geometry for all treatments. For the fourth high effective stress high pressure synthetic case, a different depth is used (Table 1 and Table 2). The fluid parameters and injection schedule are maintained constant (Table 4). The reservoir pressure and minimum principal stresses are varied for the four synthetic cases so as to represent a variation in pore pressure and resulting effective stress (Table 5).

Table 2—Reservoir Geometry for synthetic cases

Layer	Synthetic 1-3	Synthetic 4	Unit
Overlying Shale	0 – 8100	0 – 15100	(feet)
Reservoir Zone	8100 - 8230	15100 – 15230	(feet)
Underlying Shale	8230 – 1E+06	15230 – 1E+06	(feet)

Frac3D Coupled Simulation

Frac3D is used for the fracture propagation simulations. Frac3D is a 3D planar hydraulic fracture model developed to complement lumped-3D fracture modeling (Crocket, *et al*., 1986). The model is based on a finite element solution for the fracture opening and a finite difference solution for slurry transport in the fracture. In previous work detailed in Hsu et al (2012), the model had been benchmarked against data from physical laboratory tests done by Shokir and Al-Quraishy (2007). The Frac3D model was used by De Pater (2015) to match fracture geometry inferred from microseismic event clouds from the M-Site B-Sand injection. The MWX project was carried out in the Mesaverde sands of the Piceance Basin in Colorado (Warpinski et al, 1999). The M-Site fracture treatment was a prominent example of contained fracture growth in an environment where the stress contrast was insufficient to explain the observed fracture containment. The Frac3D model uses an effective stress propagation criterion rather than LEFM based stress intensity computations for fracture propagation.

The crack opening is related to fluid pressure by deriving a relation between nodal fluid pressure on a specified region and the crack width of open nodes. This relation is obtained before the simulation run and allows fast computation of crack width for a given fluid pressure distribution (Dang et al, 2009). The crack width relation is only dependent on the geomechanical parameters and layering so that it can be re-used for different pumping schedules. The potential crack area (PCA) has to be defined based on maximum fracture dimensions and this was arrived at for the four synthetic cases using a lumped 3D model. Quarter symmetry is assumed and the control volume is half of a symmetrical bi-wing fracture which is assumed symmetrical with respect to the fracture plane. The fracture propagation criterion is applied on a refined mesh near the tip, but it is still necessary to use a small mesh size for the PCA mesh in order to obtain sufficient accuracy. Different mesh sizes were tried and the final simulations used a 4ft × 4ft mesh. Even with such a relatively fine meshing, there may still be some mesh dependence because the gradient of the fracture opening near the tip will depend somewhat on the mesh size; independence of mesh size would require smooth closing of the fracture tip so that the stress singularity disappears. From the tests with the different mesh sizes, it was concluded that the size effect is relatively small compared with the effect of pore pressure variation.

Results and Discussion

Treatment Analysis

Plotting observed net pressure obtained by picking graphical Instantaneous Shut-in Pressure (ISIP) versus the closure stress obtained from G-Function plots, we see that there is a strong positive correlation. G-Function is a dimensionless time function relating shut-in time after fracture creation to total pumping time and is used to linearize pressure behavior during normal leakoff from a fracture. Barree and Mukherjee

(1996) developed idealized curve plots to aid interpretation and Barree et al (2009) summarized methods for closure stress interpretation. Figure 6 shows the treatment analysis results for the breakdown injections and Figure 8 for the minifrac injections. While the breakdown injections show a clear correlation, this is less apparent in the minifracs where fluid viscosity effects play a larger role.

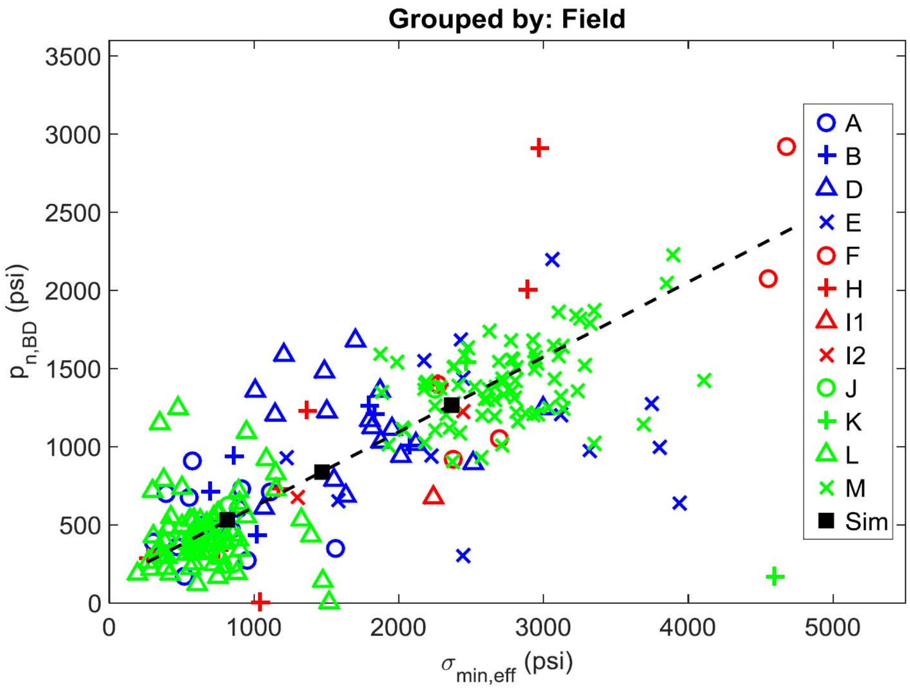

Figure 6—Net Pressure vs. Effective Stress for Breakdown Injections. The fields are indicated with letter codes and the simulations with Sim.

The presence of an intercept for observed net pressure implies a positive net pressure for an effective stress of zero, assuming a linear relation. However, this appears only significant in very shallow formations where fractures are used for civil engineering applications. In petroleum reservoirs there will always be a significant confining stress of a few hundred psi. Figure 7 shows the breakdown data averaged over the fields. The same correlation is observed, with exception of fields I1, K which had only a few data points so they are expected to show more scatter. Figure 9 shows the correlation grouped by basin and the same correlation is found, so it appears that there is no regional influence.

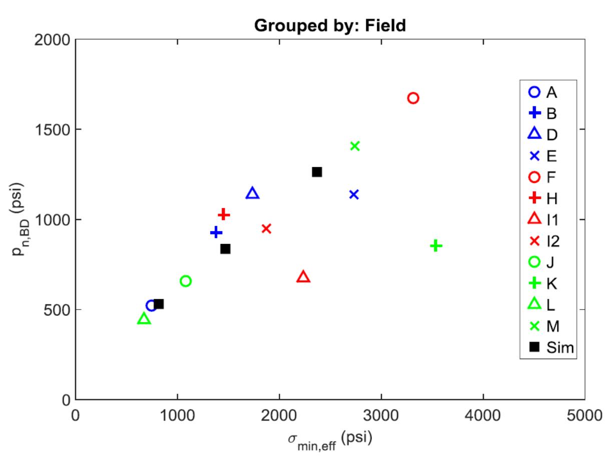

Figure 7—Net Pressure (averaged over fields) vs. Effective Stress for Breakdown Injections. The fields with the largest deviation (I2 and K) had only one or two data points.

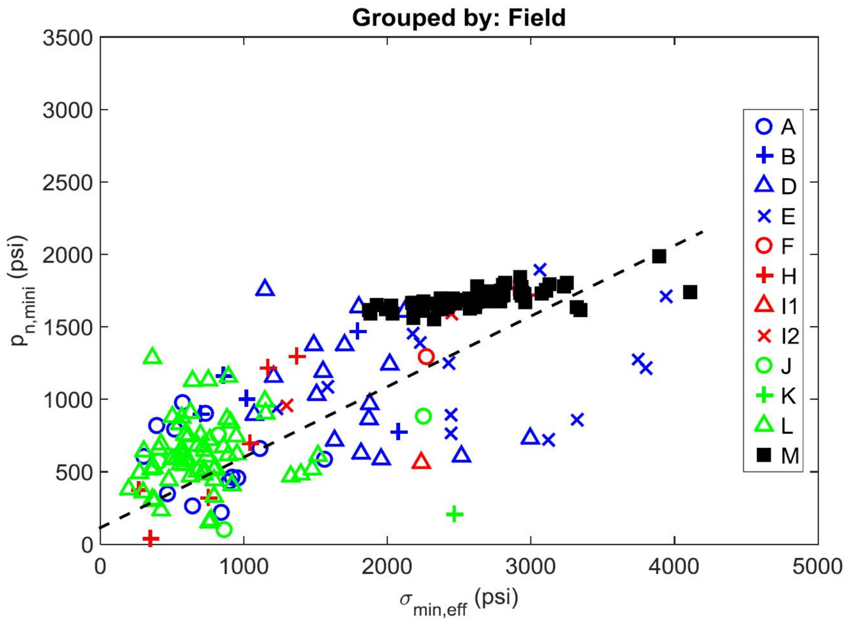

Figure 8—Net Pressure vs. Effective Stress for Minifrac Injections and the fit line from breakdown injections.

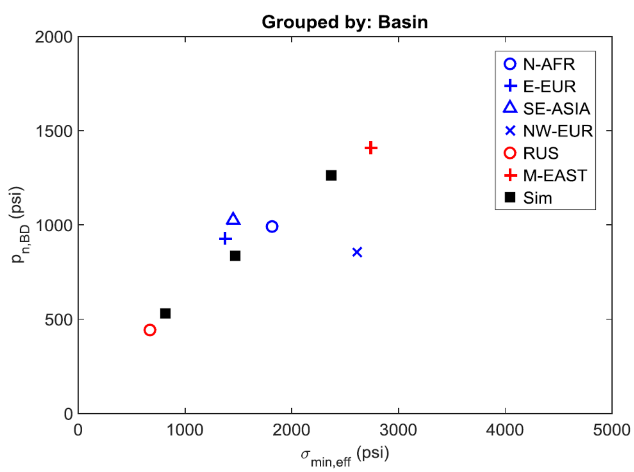

Figure 9—Net Pressure (averaged over Basins) vs. Effective Stress for Breakdown Injections.

The data also show that the ratio of the net pressure to effective stress is less than one. So, an increase in effective stress is not just added to propagation pressure. This can be expected for a non-linear system as a hydraulic fracture since other factors will also play some role in the propagation pressure.

It appears that for a wide range of reservoir parameters, the sensitivity of net pressure to effective stress is about 0.45. However, this is an average value; the model simulations match this sensitivity for a particular set of input parameters that represent the average for the entire data set. For another set of input parameters this sensitivity can be different. The scatter around the average line is fairly large, which can be expected since a sensitivity analysis with the coupled model showed that parameter variation can change net pressure by 1000 psi. In particular, increasing tensile strength and critical width has a large impact on the simulated net pressure. We used values for these parameters that are representative of laboratory measured rock strength, but at field scale these might be different. The effect of pore pressure means that a very low strength has little effect on net pressure since the effective stress will then dominate.

For the breakdown injections, the tip effect governs net pressure and the sensitivity to effective stress is determined by the choice for tensile strength.

An attempt to normalize the net pressure for differences in modulus, fluid viscosity and injection rate yielded no decrease in scatter, probably because of parameter uncertainty. That makes it the more remarkable that for the whole data set, a consistent sensitivity to effective stress level is observed. Some of the scatter is likely attributed to different sensitivity of net pressure to reservoir pressure differences, but that scatter is fairly small.

An issue with the observed correlation is that effective stress might also impact the picking of closure pressure which is often difficult from pressure fall-offs. That could introduce a systematic bias in the relation between net pressure and effective stress. The model however, shows that a similar effect is expected from a fully coupled simulation which supports that the correlation is real. Further work is needed to determine whether the observed correlation is limited to some regime of hydro-fracture propagation or that the relation is generally expected.

Coupled Simulations

Using a simple three layer geomechanical model, coupled simulations are run for the four synthetic reservoir test cases; input parameters are listed in Table 3. The net pressure and fracture geometry results are depicted in Figure 10 and Figure 11. The discontinuous parts of the curves indicate the fracture initiation pressure and geometry calculated by a pseudo 3D model. This is used as an initial input for the Frac3D simulator. From the numerical results, it is observed that a higher effective stress elevates net pressure. This is true for an effective stress increase owing to low pore pressure and also in the case when there is a large difference between pore pressure and minimum principal stress, as expected from the model formulation. The only difference would be the role of leak-off which is rather small in these cases. The fracture widths are also higher with higher effective stress. In the case of fracture dimensions, it is seen that for the lowest effective stress case i.e. the over pressured case, the fracture is longer or possesses a higher aspect ratio (fracture length to height). Increases in effective stress result in a more radial fracture geometry, as the higher net pressure gives more height growth. In all the simulations, the volume of fluid pumped was just enough to cover the pay zone. This ensures that there is no effect of fracture containment on net pressure.

Table 3—Reservoir Properties used for the Synthetic Frac3D Simulations

Reservoir Properties		
Pay Permeability	3	(mD)
Shale Permeability	0	(mD)
Pay Porosity	0.1	(−)
Shale Porosity	0.01	(−)
Pay Y-Modulus	4.50E+06	(psi)
Shale Y-Modulus	5.40E+06	(psi)
Pay Poisson Ratio	0.2	(−)
Shale Poisson Ratio	0.25	(−)
Pay tensile strength	1.45E+03	(psi)
Shale tensile strength	1.45E+03	(psi)
Pay critical width	1.20E-02	(in)
Shale critical width	1.20E-02	(in)
Reservoir Temperature	230	(F)

Table 4—Fluid Properties used for the Synthetic Frac3D Simulations

Fluid Properties		
Breakdown Fluid	WG 22	(−)
Manufacturer	Halliburton	(−)
Viscosity	4.2	(cP)
Power Law Exponent	0.557	(−)
Consistency Index	6.00E-03	(lbf s^n/ft^2)
Injection Rate	23.9	(bpm)
Injected Volume	1.20E+04	(gallons)

Table 5—Pore Pressure and Closure Stress Values for Synthetic Frac3D Simulations

	Overpressured	Hydrostatic	Underpressured	High Eff. Stress
Pore Pressure Gradient (psi/ft)	0.85	0.49	0.15	0.7
Pay Closure Stress Gradient (psi/ft)	0.96	0.67	0.44	1
Shale Closure Stress Gradient (psi/ft)	1.13	0.84	0.61	1.15
Pay Effective Stress (psi)	816	1471	2368	4550

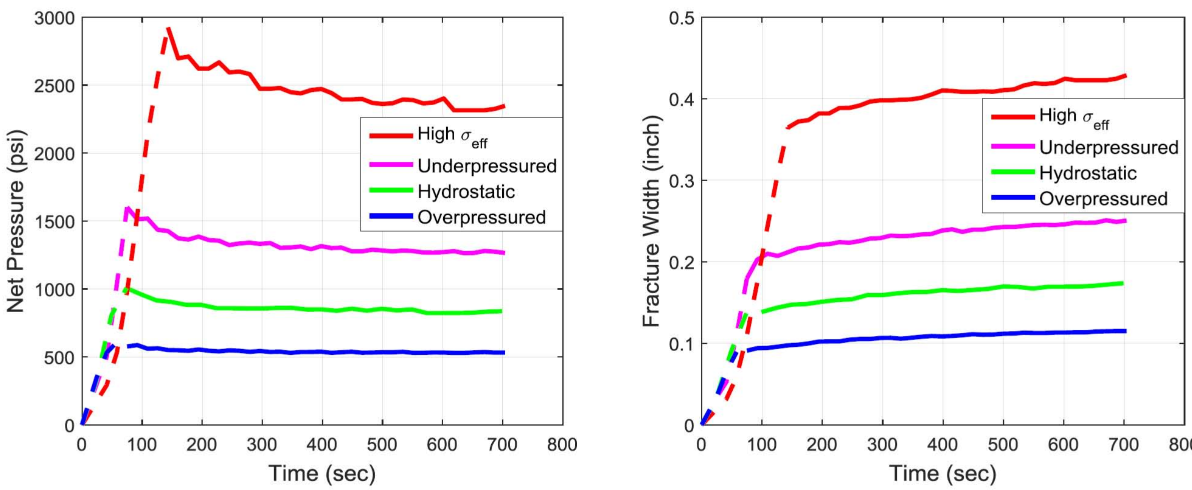

Figure 10—Coupled Simulation Results for the Synthetic Test Cases: Net Pressure (left) and Fracture Width (right)

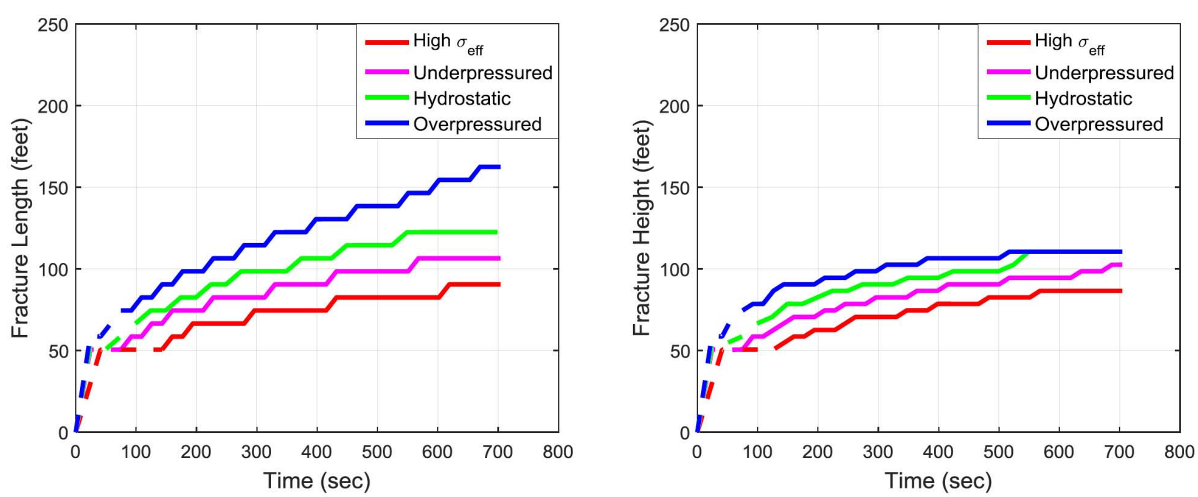

Figure 11—Coupled Simulation Results for the Synthetic Test Cases: Fracture Length (left) and Fracture Height (right).

Comparison with Fracture Treatment Data

By directly comparing the simulation results to the pressure data from the breakdown injections (see Figure 6); it can be observed that the Frac3D model net pressures match closely with the ISIP net pressure pertaining to the breakdown and minifrac injections. However the mainfrac ISIP net pressure is considerably higher and the scatter is so high that there is no discernable correlation, as shown in Figure 12. Assuming a linear fit for the range of effective stress used for the four synthetic cases, it can be observed that the breakdown injection data fits more closely and the minifrac data points exhibits more scatter.

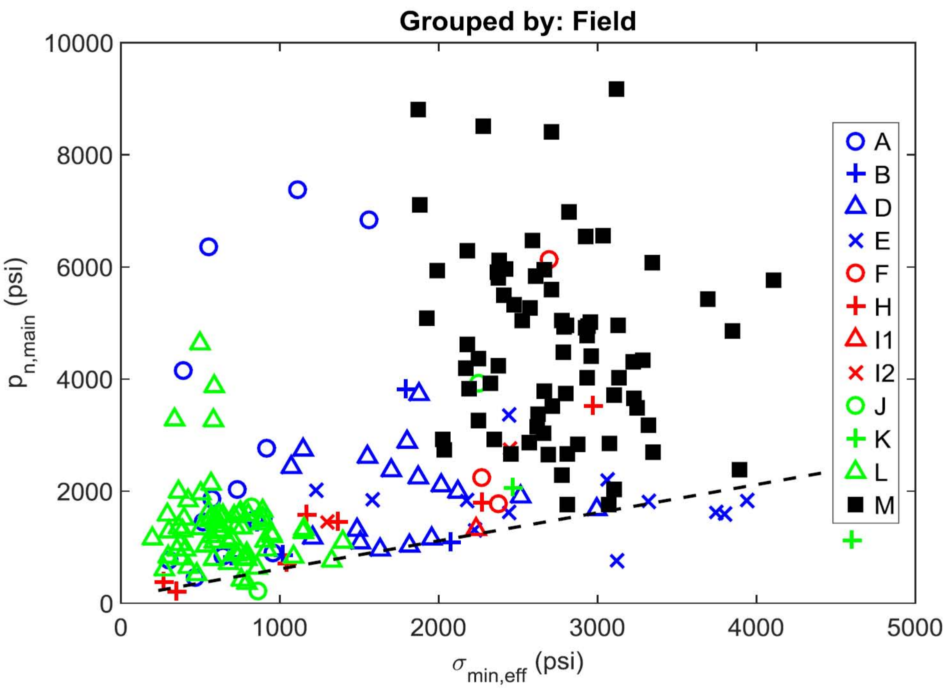

Figure 12—Comparison between Field Fracture Treatment Data and the fit line from breakdown injections.

An obvious explanation is that the viscosity of the fluid used for minifracs is much higher than for breakdown injections which are mostly performed using slick water or brine. There are multiple reasons by which the scatter in the breakdown and minifrac data can be explained. Firstly, there is uncertainty in picking the ISIP net pressure and the closure stress values. Since graphical tangent methods are used there is an element of interpretation involved. The value of effective stress corresponding to each treatment is a function of the ISIP and the closure stress and errors can be accumulated. Secondly, the database of treatments involve those in which extreme depletion have yielded inaccurate measurements of bottom hole pressure since the wells are on vacuum. Some treatments used surface gauges instead of bottom hole gauges adding to potential inaccuracy in determination of the bottom hole pressure. A third reason could be complex interplay of other factors, like multiple fracture propagation, shear decoupling and tip plasticity that dominates and hence mask the effective stress effect. A fourth reason could simply be the fact that the treatment volumes and pumping times were different for each treatment. In this case, the ISIP net pressure picked was not necessarily the end of radial growth when the fracture interacts with the stress barrier, but simply the time when injection was terminated. With a wide variety of injection volumes, some injections may have stopped when the fracture was still growing radially, and some stopped when the fracture had already become contained.

Sensitivity analysis on the normal reservoir pressure gradient case revealed that the tensile strength of the rock was an important parameter that influenced the net pressure. Though tensile strength is generally presumed to be low in rock masses, it can possibly have higher values with depth. An analysis of the slope of a linear fit line through the points obtained from the simulations indicates that the slope is the ratio of numerical net pressure to the sum of effective stress and the tensile strength. There is, therefore, a component of net pressure that is needed to maintain fracture opening at the tip and another one that maintains fluid flow within the fracture. The fracture volumes created in the simulations are small compared to viscosity dominated propped fracture treatments and the width difference is nearly four times when the over pressured and high effective stress cases are compared. This indicates that the numerical correlation of net pressure as a function of effective stress is a function of the material properties of the pay zone and is strongly related to the input tensile strength and the critical cohesive zone width. From experimental hydraulic fractures in the laboratory, it has been observed that they are toughness dominated and follow a different scaling law as compared to field scale fractures which are viscosity dominated (Detournay et al, 2007).

Discussion

There is a strong correlation between net pressure and effective stress, but this can only be clearly discerned in breakdown injections and to a lesser extent in minifracs, where other effects such as fluid viscosity also affect net pressure. On average, main treatments show much higher net pressure, with significant variation from well to well, even in the same field. This may lead to the conclusion that the effective stress effect is of little practical significance for the propped treatments. However, a more reasonable conclusion is that net pressure as measured in main treatments is strongly influenced by effects like proppant drag, banking and tip-screen-outs, and that in some cases even spurious effects like near-wellbore friction can affect the observed net pressure at shut-in. The net propagation pressure is still influenced by effective stress, but other physical mechanisms become more important once proppant is being pumped.

The latter view is supported by our experience with matching observed pressure with different models. Such exercises should yield very similar fracture geometry since all industry models are based on the same principles: elastic opening, mass balance, fluid friction and some tip pressure. Despite all the discussion of differences between the various models, the matched models should agree on the relation between pressure and geometry. However, comparing different models (with different people running the models) always yields widely different geometry for the same input. The explanation is that a lot of interpretation is needed to make sense of the observed pressure. For instance, a strongly rising pressure during the prop stages, followed by a strong decline after shut-in can be matched as a perfect tip-screen-out when the fast decline is ignored, which is sometimes warranted. If, the fast decline is included in the analysis, the interpretation leads to much less screen-out effect and assigning the pressure rise mostly to friction, that only falls off slowly after shut-in. If one takes into account such effects much of the high treatment pressure points in Figure 12 may be caused by other effects than true propagation pressure.

Accepting that most of the apparent high net pressures observed after the propped stages are related to the effects of proppant on fracture propagation leads to the conclusion that the propagation pressure for a fluid filled fracture is still governed by effective stress, which has important consequences for fracture geometry. Height growth may be affected by differences in effective stress and also the level of net pressure should be based on effective stress, if no direct observations are available. Fracture designs, based on adjusting the pad volume, are strongly dependent on the level of net pressure, which controls the fracture geometry at the point when proppant starts to enter the fracture. Current models can do a good job of modeling the *changes* in net pressure once proppant starts to affect fracture growth, but cannot do a good job of predicting the absolute level of net pressure for a fluid filled fracture. This is where the results of this work give a big advance to fracture modeling.

Currently, the best approach to fracture modeling is developing a so-called calibrated model that for a number of treatments matches directly observed fracture geometry.

Even with a sophisticated fracture model that incorporated the correct fracture propagation physics, it will be necessary to calibrate a model in view of complexities in the fracture process (for instance the exact pore pressure at the fracture tip) and lack of accurate knowledge of input parameters. The best results with such calibrated models will be obtained if the model is based on the correct physics. Incorporating the effective stress in the fracture propagation criterion will aid in developing more accurate models which will deliver better predictions of fracture geometry.

Conclusions

The results from the simulations and analysis of treatments suggest the following conclusions:

From the strong empirical correlation between net pressure and effective stress, it is evident that the effective stress law for fracture propagation is valid over a wide range of effective stresses. It is remarkable that such a correlation is observed for a wide range of reservoir permeability and elastic modulus. The scatter in the treatment data or deviations from the net pressure effective stress relationship can likely be attributed to effects of fracture complexity, fracture tip plasticity, near wellbore tortuosity and complex interactions between fluid driven fractures and pre-existing fractures.

From the numerical synthetic simulations the net pressure increase is around 45 percent of the effective stress and this closely matches with a fitted empirical correlation from the database of treatments. This fraction depends on material properties like tensile strength and the size of the cohesive zone and we ascertained this from sensitivity analysis performed by varying parameters with respect to the normally pressured reservoir synthetic test case. The sensitivity of net pressure to effective stress is therefore influenced by the choice of strength and the relatively low fluid viscosity in the breakdown injections,so that tip pressure dominates.

The relatively simple physics of pore pressure (and high effective stress) can be used to explain high net pressures observed in fracturing operations in depleted and high stressed regions. The correlation obtained can be used for fracture treatment design. The local tip pore pressure can be used as a pressure matching parameter and should be considered before applying unphysical values of modulus or fracture toughness. Accurate values of closure and pore pressure are hence useful as a predictive tool for fracture design and pressure diagnostics.

Since measured fracture dimensions from the treatment database was not available, we could not make any direct comparisons between the containment effects of pore pressure from the treatments to that predicted by the simulations. However, the simulations indicate that the magnitude of effective stress influences the fracture geometry. A higher effective stress would result in a wider, shorter and more radial fracture and lowering of the effective stress magnitude would increase the fracture aspect ratio with a smaller fracture width. It has been observed that fractures in depleted reservoirs remain constrained within pay zones and rarely exhibit fracture height growth. It can be thus be extrapolated that in addition to the effect of higher closure stresses in bounding shales (higher stress contrast) the higher effective stress owing to depletion is also playing a role in fracture containment.

Comparison between lumped 3D and Frac3D coupled simulations indicate that the lumped models in general underestimate net pressure and overestimate fracture size. Such an outcome is due to the fact that in the pseudo 3D models, pore pressure does not explicitly influence the propagation criterion but just the fluid leakoff calculation. Thus fracture models need to be based on effective stress propagation criteria with a cohesive zone description in order to represent the physics of pore pressure change. For lumped models, this correlation can still be used, qualitatively, as a way to set the level of net pressure for fracture design simulations and to match observed net pressures in the field.

Nomenclature

Units: SI (m = metre, s = second, Pa = Pascal)

Dimensions: m = mass, L = length, t = time

Variable	Description	Units	Dimensions
D_{perf} :	Depth of center of perforations	[m]	(L)
G_{min} :	Minimum Stress gradient in pay	[Pa/m]	(m/L^2t^2)
G_{res} :	Reservoir pressure gradient	[Pa/m]	(m/L^2t^2)
p_c,BD :	Closure pressure from breakdown injection	[Pa]	(m/Lt^2)
p_n,BD :	Observed net pressure in breakdown injection	[Pa]	(m/Lt^2)
$p_{n,main}$:	Observed net pressure in main frac	[Pa]	(m/Lt^2)
$p_{n,mini}$:	Observed net pressure in minifrac	[Pa]	(m/Lt^2)
$p_{n,obs}$:	Observed net pressure	[Pa]	(m/Lt^2)
σ_{min} :	Minimum horizontal stress	[Pa]	(m/Lt^2)
$\sigma_{min,eff}$:	Effective minimum horizontal stress	[Pa]	(m/Lt^2)

References

Abass, H. H., Brumley, J. L., & Venditto, J. J., 1994. Oriented Perforations - A Rock Mechanics View. In: Paper presented at the SPE Annual Technical Conference and Exhibition, New Orleans, Louisiana, 25-28 September. http://dx.doi.org/10.2118/28555-MS

Barree, R. D., Barree, V. L., & Craig, D., 2009. Holistic Fracture Diagnostics: Consistent Interpretation of Prefrac Injection Tests Using Multiple Analysis Methods. SPE Production & Operations. **24** (3), 396 - 406 http://dx.doi.org/10.2118/107877-PA

Barree, R. D., & Mukherjee, H., 1996. Determination of Pressure Dependent Leakoff and Its Effect on Fracture Geometry. In: Paper presented at the SPE Annual Technical Conference and Exhibition, Denver, Colorado, 6 – 9 October. http://dx.doi.org/10.2118/36424-MS

Behrmann, L. A., & Elbel, J. L., 1991. Effect of Perforations on Fracture Initiation. Journal of Petroleum Technology, **43** (5), 608-615. http://dx.doi.org/10.2118/20661-PA

Crockett et al. : "A Complete Integrated Model for Design and Real-Time Analysis of Hydraulic Fracturing Operations," paper SPE 15069 presented at the SPE California Regional Meeting, Oakland, CA, April 2-4, 1986.

Dam, D. B. van, & de Pater, C. J., 2001. Roughness of Hydraulic Fractures: Importance of In-Situ Stress and Tip Processes. Society of Petroleum Engineers. SPE Journal, **6**(01), 4-13,

Dam, D. B. van, Papanastasiou, P., & de Pater, C. J., 2002. Impact of Rock Plasticity on Hydraulic Fracture Propagation and Closure. SPE Dang Xinglai, Hsu.Y. 2009. Cracking Module, Internal Technical Report, Nov. 2010.

Detournay, E., Peirce, A. P., & Bunger, A. P., 2007. Viscosity-dominated Hydraulic Fractures. In: Paper presented at the 1st Canada - U.S. Rock Mechanics Symposium, Vancouver, Canada, 27-31 May. Vancouver, Canada. ARMA-07-205

Hsu, Y., X. Dang, W. Chilton, P. Chang, I. Stelin, D. Gusain, N. Northington and C.J. de Pater., 2012. New Physics-Based 3D Hydraulic Fracture Model. In: Paper presented at the SPE Hydraulic Fracturing Technology Conference, The Woodlands, Texas, USA, 6-8 February. http://dx.doi.org/10.2118/152525-MS

Nolte, Kenneth.1979. Determination of fracture parameters from fracturing pressure decline. In: Paper presented at the SPE Annual Technical Conference and Exhibition, LasVegas, Nevada, 23–26 September. http://dx.doi.org/10.2118/8341-MS

Pater, C. J. de, 2015. Hydraulic Fracture Containment: New Insights In to Mapped Geometry. In: Paper presented at the SPE Hydraulic Fracturing Technology Conference, The Woodlands, Texas, USA, 3-5 February. http://dx.doi.org/10.2118/173359-MS

Shaoul, J. R., de Pater, C. J., Al-Hashmi, M., & Langedijk, R. A., 2003. Comprehensive Fracture and Production Analysis Leads to Optimized Fracture Stimulation Strategy in a Laminated Gas/Condensate Reservoir in Oman. In: Paper presented at the SPE European Formation Damage Conference, The Hague, Netherlands. 13-14 May.

Shokir, E.M. and Al-Quraishi, A.A., 2007. Experimental and Numerical Investigation of Proppant Placement in Hydraulic Fractures. In: Paper presented at the Latin American & Caribbean Petroleum Engineering Conference, Buenos Aires, Argentina, 15-18 April. Production & Facilities, 17(03), 149-159,

Visser, J. H. M., 1998. Extensile Hydraulic Fracturing of (Saturated) Porous Materials, Doctoral Thesis, TU Delft. uuid:4d4ccf8e-f61d-436c-a8ed-19d91e8db4c5

Warpinski, N. R., T. B. Wright, J. E. Uhl, B. P. Engler, P. M. Drozda, R. E. Peterson and P. T. Branagan,. 1999., "Microseismic Monitoring of the B-Sand Hydraulic- Fracture Experiment at the DOE/GRI Multisite Project, SPE Journal, **4**(03), 242-250.

Weijers, L., 1995. The Near-Wellbore Geometry of Hydraulic Fractures Initiated from Horizontal and Deviated Wells, Doctoral Thesis, TU Delft,